

# A New Color-Magnitude Diagram for Palomar 11

Matthew S. Lewis, W. M. Liu<sup>1</sup>, N.E.Q. Paust and Brian Chaboyer

*Department of Physics and Astronomy, Dartmouth College, 6127 Wilder Lab, Hanover,  
NH 03755*

## ABSTRACT

We present new photometry for the Galactic thick disk globular cluster Palomar 11 extending well past the main sequence turn-off in the V and I bands. This photometry shows noticeable, but depleted red giant and subgiant branches. The difference in magnitude between the red horizontal branch (red clump) and the subgiant branch is used to determine that Palomar 11 has an age of  $10.4 \pm 0.5$  Gyr. The red clump is used to derive a distance  $d_{\odot} = 14.3 \pm 0.4$  kpc, and a mean cluster reddening of  $E(V - I) = 0.40 \pm 0.03$ . There is differential reddening across the cluster, of order  $\delta E(V - I) \sim 0.07$ . The colour magnitude diagram of Palomar 11 is virtually identical to that of the thick disk globular cluster NGC 5927, implying that these two clusters have a similar age and metallicity. Palomar 11 has a slightly redder red giant branch than 47 Tuc, implying that Palomar 11 is 0.15 dex more metal-rich, or 1 Gyr older than 47 Tuc. Ca II triplet observations (Rutledge et al. 1997) favour the hypothesis that Palomar 11 is the same age as 47 Tuc, but slightly more metal-rich.

*Subject headings:* Galaxy: formation — globular clusters: general — globular clusters: individual (Palomar11)

## 1. Introduction

The globular cluster Palomar 11 (Pal 11) is located at  $\alpha_{2000} = 19^{\text{h}}45^{\text{m}}14.4^{\text{s}}$ ,  $\delta_{2000} = -8^{\circ}0'26''$  ( $b = -800$ ;  $\ell = 31.81$ ) in the constellation Aquila. It sits roughly 13 kpc from the Sun and 8 kpc from the galactic center with an estimated metallicity of  $[\text{Fe}/\text{H}] = -0.4$  (Harris 1996, hereafter H96). It belongs to the population of metal-rich clusters with  $R_{GC} \gtrsim 3$  kpc

---

<sup>1</sup>present address: Department of Astronomy, University of Arizona, 933 N Cherry Ave., Tucson AZ 85721-0065

often associated with the thick disk. However, Pal 11 is located well outside the plane of the disk at  $Z = -3.5$  kpc (Cersosimo et al. 1993).

There has been only one published color magnitude diagram (CMD) for this cluster (Ortolani et al. 2001, hereafter OBB01). OBB01 did note two other unpublished CMDs from literature abstracts which derived some cluster properties for Pal 11; Cersosimo et al. (1993) and Cudworth & Schommer (1984). While these sources derive some cluster parameters (see Table 1 for a list of published values), none of them report a value for the main sequence turnoff. In this paper a new V,V-I CMD for Pal 11 with photometry reaching well past the main sequence turnoff is presented and used to determine the age of Pal 11. There are currently only 6 other thick disk clusters with age determinations (Salaris & Weiss 2002; De Angeli et al. 2005).

In Section 2 the details of the observations and photometry are discussed. In §3 we present the CMD and briefly discuss the blue straggler population, §4 determines the cluster parameters, such as distance, reddening, metallicity, and age. Finally, §5 discusses these findings.

## 2. Observations & Photometric Calculations

Observations of Palomar 11 were obtained over five nights from September 4 to September 8, 1999 with the 2.4m Hiltner telescope at the MDM Observatory at Kitt Peak. All of the images were taken on a 2048x2048 CCD, though the image only covers 1760x1760 pixels to accommodate a 2 inch filter wheel. The images were taken at a scale of 0.275 arcsec per pixel for a field of view of 8' square. Table 2 shows a complete list of observations.

Since the tidal radius of the cluster (9.8'; H96) is comparable to the image size, observations include images centered on the cluster as well as images offset a little more than 5' South. This offset field is used to estimate the field star contamination. Figures 1 and 2 are 1200s images in the V filter of Pal 11 and the offset field.

The image reductions were all done in IRAF<sup>1</sup> with its ccdproc routine. ALLSTAR and DAOPHOT (Stetson 1987, 1994) were used in a standard manner to do crowded field photometry and extract instrumental magnitudes. All of images were matched and the coordinates of all stars were shifted onto a common coordinate system. To make our final

---

<sup>1</sup>IRAF (Image Reduction and Analysis Facility) is distributed by the National Optical Astronomy Observatory (NOAO), which is operated by the Association of Universities for Research in Astronomy, Inc., under contract with the National Science Foundation (NSF).

photometry list we require that a star be detected in a minimum of 2 V and 2 I images. We find a total number of 6675 stars with V and I magnitudes.

Since none of the nights were photometric, we matched our stars to those of OBB01 to determine the photometric transformations. Matches were found for 583 stars, with  $13 < V < 20.6$  and  $0.5 < V - I < 2.6$ . Our mean photometric errors in the matched stars are 0.024 mag in V. Fortunately, there are no apparent trends in the residuals between our photometry and the OBB01 photometry as a function of magnitude or colour. A plot of the magnitude residuals is shown in Figure 3. The bulk of the stars in the match had  $16 < V < 19.5$  and  $0.9 < V - I < 1.5$  and it would be difficult to detect residual trends with magnitude or colour outside these ranges. As a result, our photometric calibration is more uncertain for stars outside this magnitude and color range. Fortunately, the bulk of the Pal 11 stars fall within this restricted magnitude and colour range.

Our photometry is presented in Table 3. The error in the photometry is based on the frame-to-frame variation in magnitude. The origin of the pixel reference frame is located in the Southwest corner of the cluster frames.

### 3. Color-Magnitude Diagram & Observational Parameters

Figure 4a shows the V,V-I CMD of all stars in our observations, Figure 4b shows the CMD of the stars within the half-mass radius ( $2'$ ; H96) of the cluster's center ( $X=800$  &  $Y=820$ ) and Figure 4c shows the CMD of the stars located in the equivalent area to the cluster center CMD but from regions on our image which are located farthest from the cluster center. The center of the cluster was found by simply determining the peak in the star counts in the X and Y directions. The main sequence, turn-off, and subgiant branch (SGB) are all clearly visible in both. The red giant branch (RGB) and the extremely red horizontal branch (hereafter red clump or RC) are also visible, but not as well populated. The fit to the RGB is overlaid on figure 4b (see section 4.1).

The RC is sloping, which is an indication of differential reddening. To examine this, we examined the color of the turn-off as a function of position for stars in an annulus between  $1'$  to  $2'$  of the cluster center. The turn-off was found to be reddest NorthEast of the cluster center, with a variation in turn-off colour of  $V - I = 1.00$  to  $1.07$  from the SouthWest to the NorthEast of the cluster center.

The observational parameters of this CMD are presented in Table 4. In this table,  $V_{RC}$  and  $I_{RC}$  are the apparent V and I magnitudes for the RC,  $(V - I)_g$  is the (V-I) color of the RGB at the height of the RC,  $V_{SGB}$  is the apparent V magnitude of the SGB, 0.05 dex

redder than the main sequence turnoff (Chaboyer et al. 1996), and  $V_{\text{TO}}$  and  $(V - I)_{\text{TO}}$  are the apparent  $V$  magnitude and color of the main sequence turnoff. These quantities were derived using the mode of the magnitude or colour distribution for a given quantity. Given that the cluster is centrally concentrated and has differential reddening, these modal values provide an estimate of the various photometric quantities at the cluster center.

To estimate the field star contamination in the cluster CMD, star counts were made within  $2'$  of the cluster center and an equivalent area in the farthest corners from the cluster center. This ‘background’ area starts  $5.2'$  from the cluster center, so likely contains some cluster stars. Within  $2'$  of the cluster center, there are 2670 stars, while there are 457 in the background area. This gives a maximum field star contamination of 17%. Due to crowding, the photometry near the cluster center is not as deep or complete. Restricting the star counts to  $V < 22$ , there are 1561 stars within  $2'$  of the center and 226 stars in the background region, yielding a maximum field star contamination of 15%.

The blue straggler population of Pal 11 can be estimated in a similar manner. The photometric error in  $V$  and  $(V-I)$  is used to define the blue straggler region in the CMD as stars with magnitudes brighter than  $V_{\text{SGB}} + 3\sigma$  and with colors bluer than  $(V - I)_{\text{TO}} - 1\sigma$ . These values are  $V_{\text{BS}} = 20.4$  and  $(V - I)_{\text{BS}} = 0.93$ . This box is extended to half a magnitude below the RC ( $V = 17.99$ ) and to  $V - I = 0.5$  in color (see Figure 4b). In this region of the CMD, there are 44 stars within  $2'$  of the cluster center and 13 in the background region. Thus, about one-third of the stars in the blue straggler region are field stars, yielding an estimated number of blue stragglers of  $31 \pm 7$ . For comparison, there are 20 RC stars within  $2'$  of the cluster center and 1 star in the region of the RC in the background field. This yields a fraction of blue straggler stars of  $F_{\text{BSS}} \equiv N_{\text{BS}}/N_{\text{RC}} = 1.6 \pm 0.8$ . The blue straggler fraction within a globular cluster is a function of the integrated cluster luminosity (Piotto et al. 2004). Pal 11 has an integrated absolute visual magnitude of  $M_V = -7.0$ , using the integrated visual magnitude of  $V_t = 9.8$  from H96 and the distance modulus derived in §4.1. For its luminosity, Pal 11 has a high blue straggler population compared to other globular clusters (Piotto et al. 2004).

## 4. Cluster Properties

### 4.1. Distance & Reddening

The distance and reddening to Pal 11 can be estimated from the apparent magnitude of the red clump ( $V_{\text{RC}}$ ) using the method described by Alves et al. (2002). We determine  $M_V^{\text{RC}}$  and  $M_I^{\text{RC}}$ , using the Hipparcos parallax calibration combined with a correction for the

differences in age and metallicity ( $\Delta M_\lambda$ ) between our stars and the Hipparcos calibration stars (Girardi & Salaris 2001). These values depend on metallicity, so calculations were made at both  $[\text{Fe}/\text{H}] = -0.7$  and  $[\text{Fe}/\text{H}] = -0.4$  to compare with the range of previously published values. Above an age of 9 Gyr,  $\Delta M_\lambda$  has a negligible age dependence, so we assume an age greater than 9 Gyr to determine corrections (see section 4.3 for a discussion of age). These calculations yield values of  $M_V^{\text{RC}} = 0.62$ ;  $M_I^{\text{RC}} = -0.28$  for  $[\text{Fe}/\text{H}] = -0.7$  and  $M_V^{\text{RC}} = 0.75$ ;  $M_I^{\text{RC}} = -0.21$  for  $[\text{Fe}/\text{H}] = -0.4$ .

Assuming a standard extinction law (Alves et al. 2002) the following are derived:  $(m - M)_V = 16.77 \pm 0.07$ ,  $(m - M)_I = 16.38 \pm 0.04$ ,  $A_V = 1.05 \pm 0.06$ ,  $A_I = 0.61 \pm 0.04$ ,  $E(V - I) = 0.40 \pm 0.03$ ,  $E(B - V) = 0.31 \pm 0.03$ , and  $d_\odot = 14.3 \pm 0.4$  kpc. These numbers are in general agreement with other numbers published in the literature, although our reddening is slighter lower and distance slightly higher than previous estimates (see Table 1).

## 4.2. Metallicity & Reddening

The metallicity of Pal 11 has been determined using spectroscopy of the Ca II triplet (Armandroff et al. 1992). The index used is the reduced equivalent width of the calcium lines for RGB stars in a cluster, denoted  $W'$  (Rutledge et al. 1997). However the current error bars for Pal 11 are significant, with  $W' = 4.77 \pm 0.22$ . In terms of metallicity, this gives roughly  $[\text{Fe}/\text{H}] = -0.7 \pm 0.2$  based on the updated calibration of  $W'$  by Kraft & Ivans (2003). Two clusters with a similar Ca II index are 47 Tuc and NGC 5927, with  $W' = 4.53 \pm 0.05$ , and  $W' = 4.85 \pm 0.06$ , respectively. These two clusters likely bracket Pal 11 in metallicity.

The color of the RGB depends primarily on metallicity and reddening, with a smaller dependance on age. This fact has been used by Sarajedini (1994) to develop a method to simultaneously determine  $[\text{Fe}/\text{H}]$  and  $E(V-I)$ , using indicators based on the RGB color and slope. This method requires a polynomial fit to the RGB. The fit was determined using a two-step process. First, a rough fiducial was determined by eye. A standard third-order polynomial fit (with no weighting) was then made to stars which were within 0.10 in V-I of this fiducial and which do not belong to the RC. This leads to the following fit to the RGB

$$V - I = 31.49 - 4.34 * V + 0.207 * V^2 - 0.0033 * V^3. \quad (1)$$

This fit is superimposed on the data in Figure 4b.

Using this equation and following the procedure outlined by Sarajedini (1994) and the updated calibrations of Saviane et al. (2000) based on the Carretta & Gratton (1997) metallicity scale, the metallicity and reddening of Pal 11 are determined. For this purpose, the mean magnitude of the red clump is used as the magnitude of the horizontal branch.

We derive a metallicity of  $[\text{Fe}/\text{H}] = -0.76$  and a reddening of  $E(V - I) = 0.34$ . This implies  $E(B - V) = 0.27$ . These same methods were applied to photometry for 47 Tuc (Kaluzny et al. 1998) and NGC 5927 (Feltzing & Gilmore 2000). For 47 Tuc we derive a metallicity of  $[\text{Fe}/\text{H}] = -0.76$  and a reddening of  $E(V - I) = -0.02$ . For NGC 5927 we get  $[\text{Fe}/\text{H}] = -0.77$  and a reddening of  $E(V - I) = 0.55$ . These reddenings are universally lower than published values, and so suggests that the derived reddening values may not be reliable. It is not clear why the derived reddenings are lower than previous estimates, but could be related to the fact that the clusters studied here are all of relatively high metallicity, and the empirically calibration of the colour of the RGB as a function of reddening and metallicity may not be reliable for these high metallicity clusters.

The derived metallicities are the same for the three clusters. However, 47 Tuc was the most metal rich cluster used to calibrate this method. The metallicity derived for NGC 5927 is lower than that inferred from the Ca II index  $[\text{Fe}/\text{H}] = -0.64$  (Rutledge et al. 1997); and from Fe measurements based upon Fe II lines  $[\text{Fe}/\text{H}] = -0.67$  (Kraft & Ivans 2003). It is considerably lower than that determined by Zinn & West (1984),  $[\text{Fe}/\text{H}] = -0.37$ .

Thus, it appears that one cannot extrapolate the method of Sarajedini (1994) past the metallicity of 47 Tuc. It is quite possible that Pal 11 is as metal-rich as NGC 5927.

### 4.3. Cluster Age

Stellar evolution tracks were constructed using stellar evolution code described by Chaboyer et al. (1999, 2001) for masses in the range of  $0.5 M_{\odot}$  to  $2.0 M_{\odot}$  in increments of  $0.05 M_{\odot}$ . The models include the diffusion of helium and heavy elements. A solar calibrated model was calculated yielding  $Z_{\odot} = 0.02$  and  $Y_{\odot} = 0.275$  (initial abundances). For other metallicities,  $dY/dZ = 1.5$  was assumed (corresponding to a primordial helium abundance of  $Y_{BBN} = 0.245$ ). The solar calibrated mixing length was used for all the models. The transformation from the theoretical temperatures and luminosities to observed colors and magnitudes was completed using the Vandenberg & Clem (2003) color tables.

For these isochrones, the magnitude of the SGB, 0.05 magnitudes redder than the turnoff was used to calculate the difference in magnitude between the SGB and the semi-empirical  $M_V^{\text{RC}}$  determined above. This gives us  $\Delta V(\text{SGB} - \text{RC})$  as a function of age at two different metallicities (see Table 5). From Table 5, it is clear that  $\Delta V(\text{SGB} - \text{RC})$  has little sensitivity to metallicity over the range  $[\text{Fe}/\text{H}] = -0.4$  to  $-0.7$  and so can provide a robust estimate of the age of Pal 11 even though its metallicity is not well constrained. For Pal 11,  $\Delta V(\text{SGB} - \text{RC}) = 3.15 \pm 0.04$ , which gives it an estimated age of  $10.4 \pm 0.5$

Gyr. For comparison, 47 Tuc and NGC 5927 were analyzed in the same manner yielding  $\Delta V(\text{SGB} - \text{RC}) = 3.16 \pm 0.04$  and  $\Delta V(\text{SGB} - \text{RC}) = 3.15 \pm 0.04$ , corresponding to ages of  $10.6 \pm 0.5$  and  $10.4 \pm 0.5$  Gyr respectively.

Figures 5a & 5b show the CMD of Pal 11 with the CMDs of 47 Tuc and NGC 5927 overlaid, respectively. The CMDs of the two comparison clusters are shifted in color to match the turnoff color and in V magnitude to match the SGB of Pal 11. The RGBs and the RCs of Pal 11 and NGC 5927 overlap, suggesting that they are similar in age and metallicity. On the other hand, 47 Tuc has a slightly bluer RGB suggesting a different age or metallicity (or both).

To estimate the implied age and/or metallicity difference, the difference in color between the main sequence turnoff and the base of the RGB as a function of age and metallicity ( $\Delta(V - I)$ ) was measured in the isochrones. This index is sensitive to age and metallicity (Sarajedini & Demarque 1990; Vandenberg et al. 1990). The base of the RGB is defined as the point where a straight line fit to the RGB crosses the measured value of  $V_{\text{SGB}}$  as measured above. These theoretical values are compared to the observed data. Pal 11 has  $\Delta(V - I) = 0.17$  and 47 Tuc has  $\Delta(V - I) = 0.16$ , respectively. Based upon the isochrones, this difference implies that Pal 11 is 1 Gyr older or 0.15 dex more metal rich than 47 Tuc.

## 5. Summary

A new CMD for Pal 11 has been presented which reaches roughly 4 magnitudes past the main sequence turnoff. Using the magnitude of the RC, and the method of Alves et al. (2002) leads to a distance of  $d_{\odot} = 14.3 \pm 0.4$  kpc and a mean reddening of  $E(V - I) = 0.40 \pm 0.03$ . These values are in general agreement with previously published values. There is differential reddening across cluster, such that stars in the NorthEast of the cluster are approximately 0.07 mag redder in  $V - I$  than stars in the SouthWest part of the cluster. Following the method of Sarajedini (1994), we find that Pal 11 has a similar metallicity to the metal rich clusters 47 Tuc and NGC 5927.

Using the difference in magnitude between the SGB and RC, an age of  $10.4 \pm 0.5$  Gyr is determined for Pal 11. This is the first age estimate for Pal 11. Very similar ages are found for 47 Tuc and NGC 5927. After shifting to a common reddening and distance modulus, the CMDs of Pal 11 and NGC 5927 are nearly identical, which implies that these clusters have the same age and metallicity. In contrast, the RGB of 47 Tuc is slighter bluer than the Pal 11 RGB. This implies that Pal 11 and 47 Tuc must differ in age by 1 Gyr or in metallicity by 0.15 dex. Given that the CMDs of NGC 5927 and Pal 11 are very similar and NGC 5927

has a higher Ca II triplet equivalent width than 47 Tuc, it is likely that Pal 11 has a similar age to 47 Tuc, but is slightly more metal-rich. In agreement with previous studies (Salaris & Weiss 2002; De Angeli et al. 2005) we find no evidence for an age dispersion among the thick disk clusters in the Milky Way. This suggests that the stars in the thick disk clusters formed over a relatively short time-scale ( $\lesssim 500$  Myr).

We thank S. Ortolani for the electronic version of his Pal 11 photometry and the anonymous referee whose comments improved the presentation of this paper. Research supported in part by a NSF CAREER grant 0094231 to BC. BC is a Cottrell Scholar of the Research Corporation.

## REFERENCES

- Alves, D. R., Rejkuba, M., Minniti, D., & Cook, K. H. 2002 ApJ, 573, L51
- Armandroff, T. E., Da Costa, G. S., Zinn, R. 1992, AJ, 104, 164
- Catena, R. & Schommer, R. A., 1978, IAUS, 80, 177
- Carretta, E. & Gratton, R., 1997 A&AS 121, 95
- Cersosimo, S., Lydon, T. J., Sarajedini, A., & Zinn, R. 1993, BAAS, 182, 5007
- Chaboyer, B., Demarque, P., Kernan, P., Krauss, L., & Sarajedini, A., 1996, MNRAS, 283, 683
- Chaboyer, B., Green, E. M., & Liebert, J. 1999, AJ, 117, 1360
- Chaboyer, B., Fenton, W. H., Nelan, J. E., Patnaude, D. J., & Simon, F.E. 2001, ApJ, 562, 521
- Cudworth, K. M., & Schommer, R. 1984, PASP, 96, 786
- De Angeli, F., Piotto, G., Cassisi, S., Busso, G., Recio-Blanco, A., Salaris, M., Aparicio, A., & Rosenberg, A. 2005, AJ, 130, 116
- Feltzing, S., & Gilmore, G. 2000, A&A, 355, 949
- Girardi, L., Salaris, M., 2001, MNRAS, 323, 109
- Harris, W. E. 1996, AJ, 112, 1487

- Kaluzny, J., Wysocka, A., Stanek, K. Z., & Krzeminski, W. 1998, *Acta Astronomica*, 48, 439
- Kraft, R., & Ivans, I., 2003, *PASP*, 115, 143
- Ortolani, S., Bica, E., & Barbuy, B. 2001, *A&A*, 374, 564
- Piotto, G., et al. 2004, *ApJ*, 604, L109
- Rutledge, G., Hesser, J., Stetson, P., 1997, *PASP*, 109, 907
- Salaris, M., Weiss, A. 2002, *A&A*, 388, 492
- Sarajedini, A., 1994, *AJ*, 107, 618
- Sarajedini, A., & Demarque, P. 1990, *ApJ*, 365, 219
- Saviane, I., Rosenberg, A., Piotto, G., Aparicio, A. 2000, *A&A*355, 966
- Stetson, P. B. 1994, *PASP*, 106, 250
- Stetson, P. B. 1987, *PASP*, 99, 191
- VandenBerg, D. A., Bolte, M., & Stetson, P. B. 1990, *AJ*, 100, 445
- VandenBerg, D. A., & Clem, J. L. 2003, *AJ*, 126, 778
- Webbink, R. F. 1985 in *Dynamics of Star Clusters* ed. J. Goodman, & P. Hut (Dordrecht: Reidel), IAU Symp., 113, 541
- Zinn, R. 1985, *ApJ*, 293, 424
- Zinn, R. 1984, *ApJS*, 55, 45

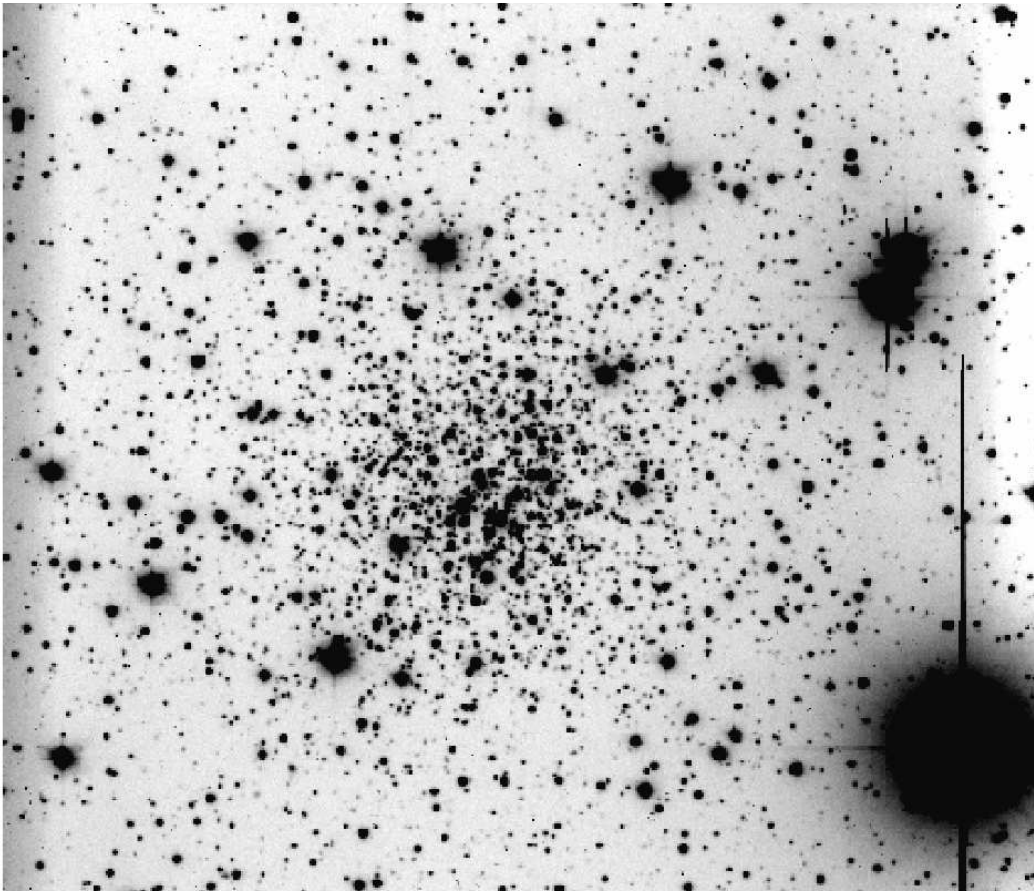


Fig. 1.— Palomar 11 in the V filter. This image is  $484''$  square, with North to the right and East up.

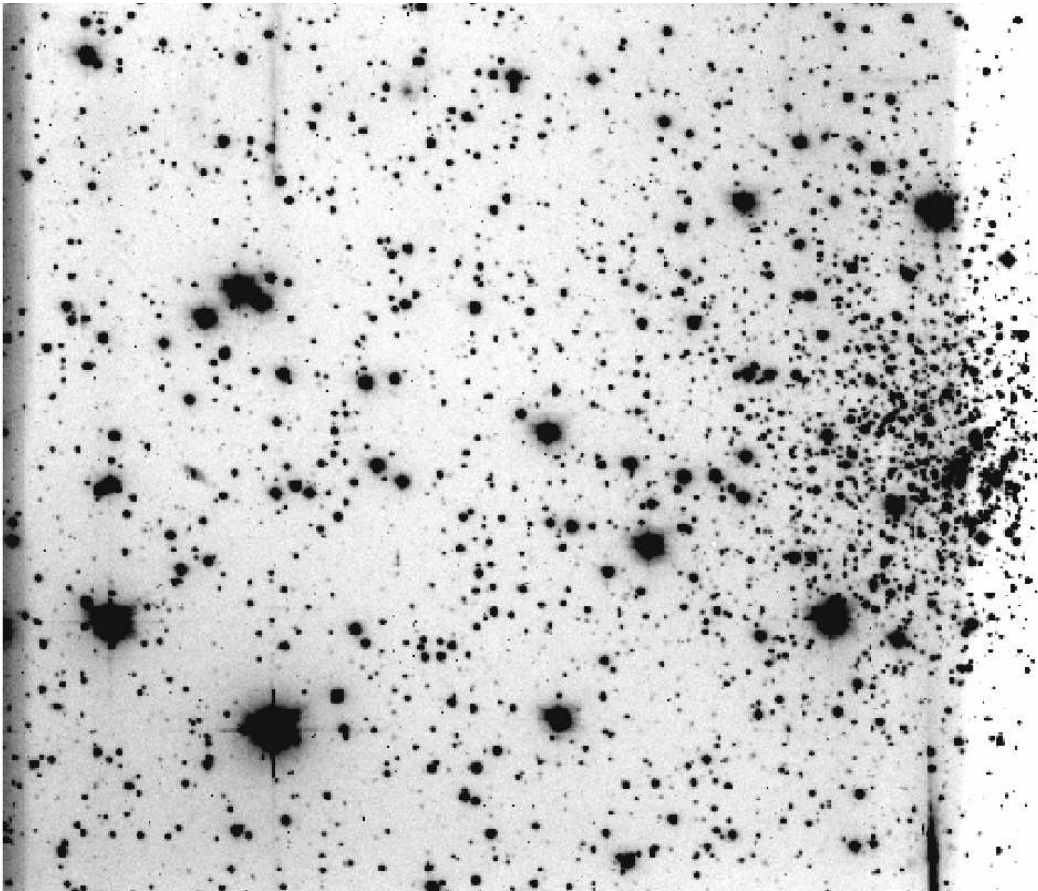


Fig. 2.— The offset field in the V filter. This image is  $484''$  square, with North to the right and East up.

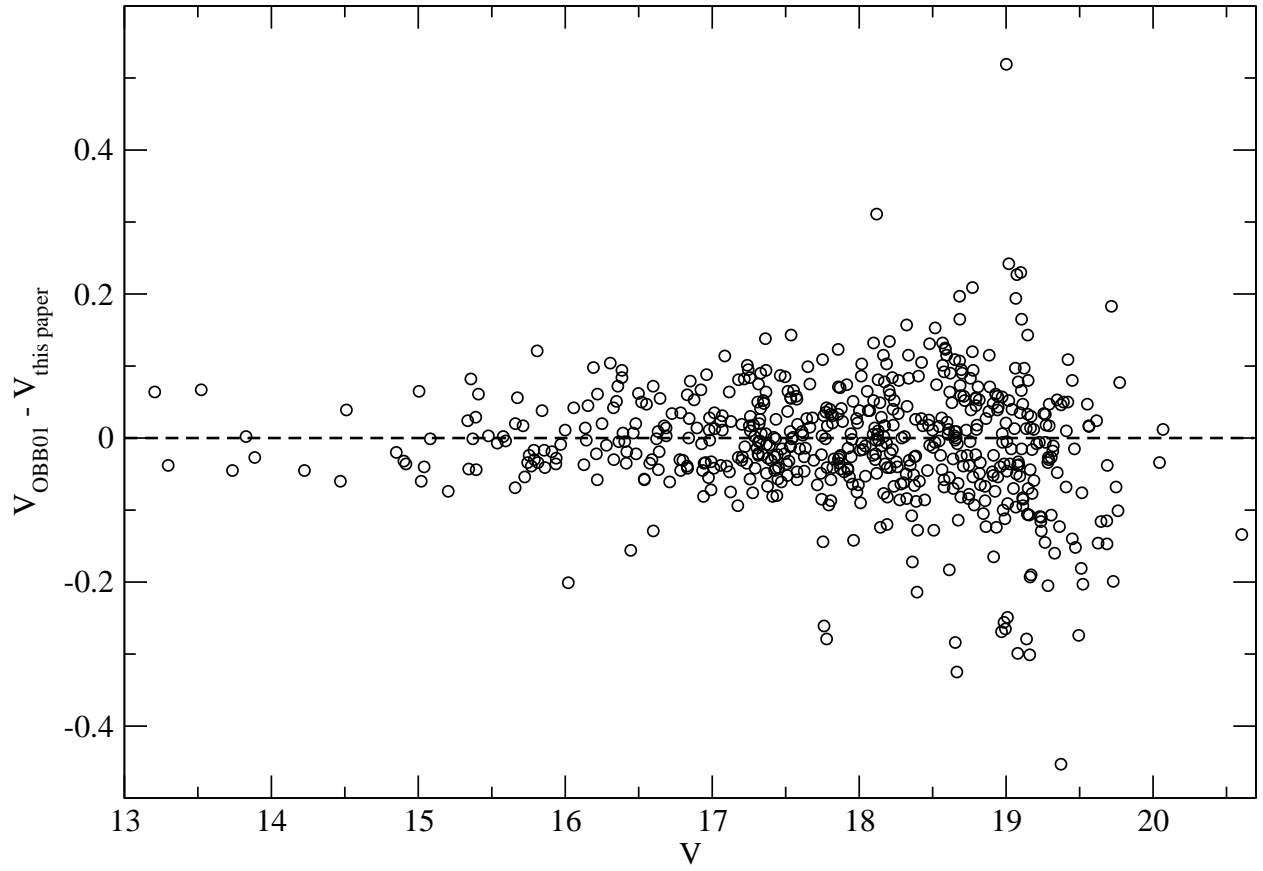


Fig. 3.— The residuals in the matched V photometry between this paper and the photometry in OBB01.

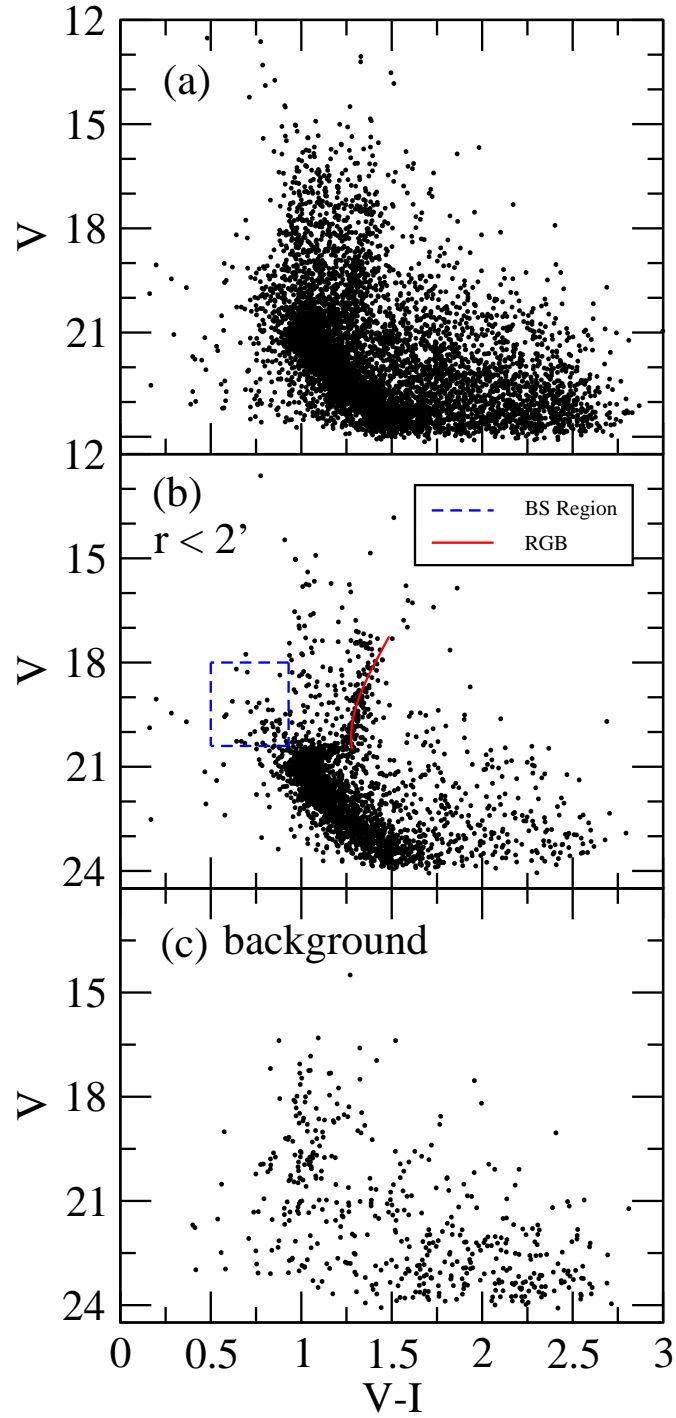


Fig. 4.— Figure (a) shows the CMD for all of the stars in the field of Palomar 11 and the offset field. Figure (b) shows only the stars within  $2'$  from the center of the cluster and contains the fit to the RGB and a box defining our BS region. Figure (c) shows the stars in an equivalent area to the cluster center field, but located in the corners of the image furthest from the cluster center.

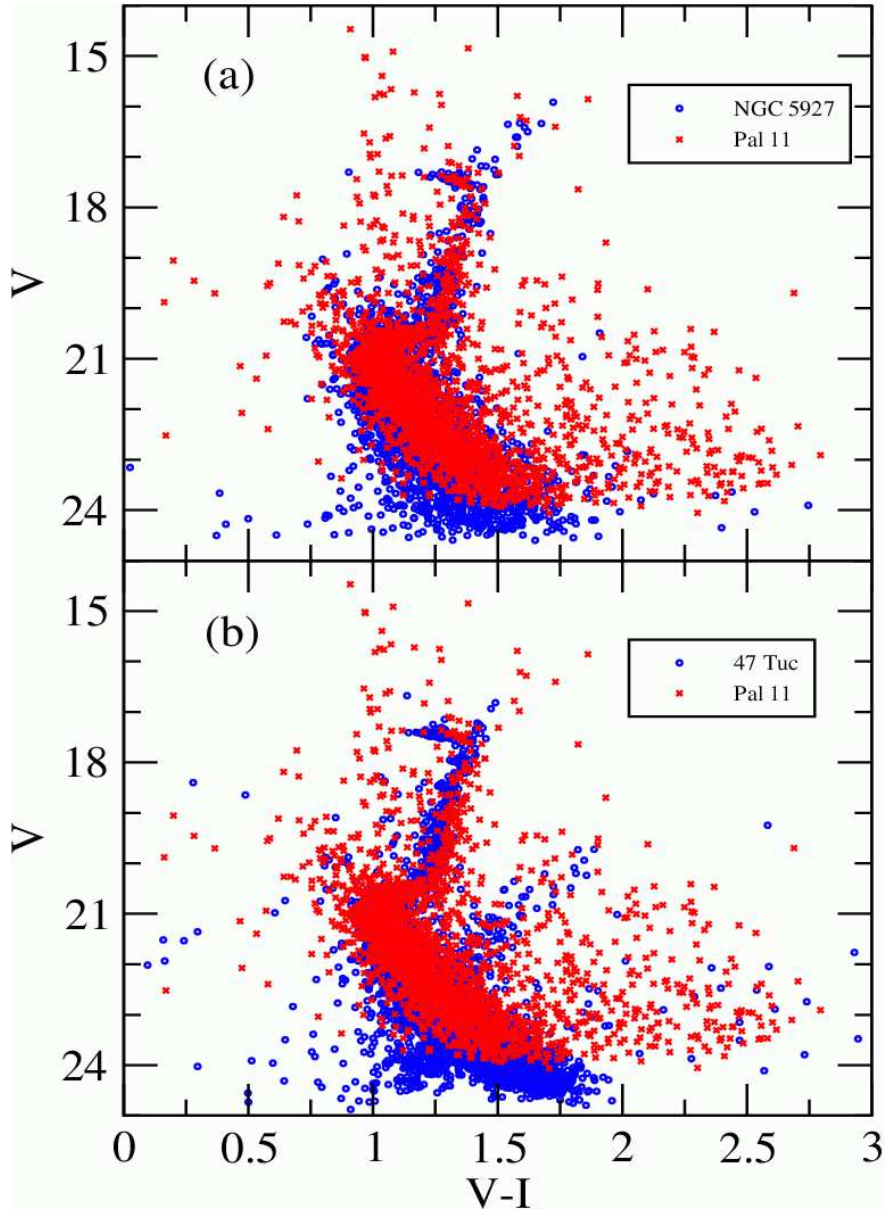


Fig. 5.— Figure (a) shows the CMDs of Pal 11 and NGC 5927, with the data from NGC 5927 shifted so that the color of the turn-off and magnitude of the SGBs coincide. Similarly, Figure (b) shows the CMDs of Pal 11 and 47 Tuc.

Table 1. Published Palomar 11 Parameters.

Paper	$V_{\text{HB}}$	$E(B - V)$	$[\text{Fe}/\text{H}]$	$d_{\odot}$
OBB01	17.4	0.35	-0.7	13.2
H96	17.40	0.35	-0.39	13
CER93	17.35	-	-0.23	-
ADZ92	-	-	$>-0.6$	-
W85	17.38	0.34	$-0.92^{\dagger}$	13.8
Z85		0.35	-0.7	-
CS84	17.3	0.34	-	12.9

<sup>†</sup>This metallicity is  $[\text{M}/\text{H}]$  rather than  $[\text{Fe}/\text{H}]$

Note. — (Ortolani et al. 2001; Harris 1996 from the February 2003 on-line edition; Cersosimo et al. 1993; Armandroff et al. 1992; Webbink 1985; Zinn 1985; Cudworth & Schommer 1984)

Table 2. Log of Observations.

Target	Date	Filter	Time(s)	Number	FWHM(")
Pal 11	9/4/99	I	20	3	1.2
	"	I	120	3	1.1
	"	I	900	2	1.4
	"	V	20	3	1.1
	"	V	200	3	1.0
	"	V	1200	3	1.4
	9/5/99	I	15	1	0.8
	"	I	900	4	1.3
	"	V	1200	1	1.4
	"	V	229	1	1.3
	9/6/99	I	20	1	1.2
	"	V	20	1	1.3
	9/7/99	V	20	1	1.2
	"	V	1200	2	1.3
Offset	9/6/99	I	20	4	1.3
	"	I	120	4	1.3
	"	I	900	3	1.3
	"	V	20	3	1.2
	"	V	200	4	1.4
	"	V	1200	2	1.2
	9/7/99	I	900	3	1.0
	"	V	1200	3	1.3

Table 3. Photometry of Palomar 11

Number	X pixel	Y pixel	V	$\delta V^*$	I	$\delta I^*$
1	-617.12	-49.09	18.687	0.018	17.510	0.028
2	-239.37	-47.76	22.975	0.079	20.921	0.052
3	-450.70	-44.58	20.349	0.018	19.267	0.016
4	-760.36	-43.60	19.955	0.011	18.937	0.015
5	704.18	-42.28	22.573	0.051	20.493	0.032

\*These errors are determined by the frame to frame variation in V or I

Note. — A full table of photometry can be found in the electronic version of this article

Table 4. Palomar 11 Parameters.

Parameter	Value
$V_{\text{RC}}$	$17.46 \pm 0.03$
$I_{\text{RC}}$	$16.14 \pm 0.03$
$(V - I)_{\text{g}}$	$1.43 \pm 0.02$
$V_{\text{SGB}}$	$20.61 \pm 0.02$
$V_{\text{TO}}$	$20.88 \pm 0.06$
$(V - I)_{\text{TO}}$	$1.03 \pm 0.01$

Table 5. Theoretical  $\Delta V(\text{SGB-RC})$

Age (Gyr)	$\Delta V(\text{SGB-RC})$	
	[Fe/H]=−0.4	[Fe/H]=−0.7
9	3.002	2.989
10	3.114	3.104
11	3.218	3.189
12	3.304	3.278
13	3.385	3.358
14	3.461	3.443
15	3.532	3.508